Porous field emission devices based on polyimide membranes using diode and triode configurations

V. P. Mammana
Instituto de Física, Universidade de São Paulo, São Paulo, Brazil

L. R. C. Fonseca
Motorola, DigitalDNA Laboratories, Mesa, Arizona

A. Pavani Filho
Instituto Nacional de Tecnologia da Informatica, Campinas, São Paulo, Brazil

O. R. Monteiro
Lawrence Berkeley Laboratory, University of California, Berkeley, California 94720

R. Ramprasad
Motorola, DigitalDNA Laboratories, Tempe, Arizona

P. von Allmen
Motorola, Flat Panel Display Division, Tempe, Arizona

Residual gas inside field emission displays (FED) is the most important issue related to the device lifetime. Increasing the display area while maintaining the display thickness unchanged results in lifetime decrease, since the pressure gradient is fostered. Therefore, improvement of vacuum properties is a mandatory step towards large area displays. In a prior publication we have demonstrated that porous diamond membranes show good vacuum performance, while requiring low emitter switching voltage. In this work, we continue the porous membrane development by using polyimide as the base material for the membrane. The use of polyimide instead of diamond allows for easier production of large area porous FEDs. In addition, we present results of preliminary field emission experiments showing a direct correlation between the emitted current and the number of pores. This result strongly suggests that the emission sites are located at the pore edges in the polyimide membranes, similar to our observations for diamond membranes. From the theoretical point of view, we propose a new geometry, still based on the use of pores, but including a grid for triode mode operation. Finally, we present electron trajectory simulations that address some of the focusing issues in the proposed device. © *2001 American Vacuum Society.*
[DOI: 10.1116/1.1350838]

I. INTRODUCTION

Field emission displays (FED) are ideally suited to face the numerous challenges of producing high quality and low cost large area flat panel displays.[1] The FED technologies chosen in most industrial programs are at very diverse stages of development. FEDs based on Spindt-tip cathodes should reach the market within months, while technologies based on carbon materials as field emitters still require a number of years of development. Despite the advanced state of readiness, the search for new designs and materials for the production of FEDs is of considerable importance, since it contributes to the technological evolution towards new generations of products. The consumer goods market, continuously requires lower costs, smaller power consumption, larger areas, higher image resolution and quality, longer lifetime, and enhanced robustness (e.g., mechanically flexible). Consequently, the industry has to be prepared to supply this demand in an appropriate timeframe.

The move to large area processing is challenging in itself because of uniformity and reproducibility issues. However, in the case of FEDs, the increase in area poses one additional difficulty, namely the increase in the gas load from a large degassing area together with a small effective pumping speed.[2–4] In order to promote a higher pumping speed, a significant increase in device area needs to be accompanied by a larger vacuum conductance, which can only be achieved by increasing the anode–cathode separation. This increase leads to a series of technical difficulties, including defocusing of the electron beam, the need of tall spacers, and mechanical stress as well as alignment issues. If the cathode–anode separation is not increased, the low vacuum conductance results in large pressure gradients and higher local pressures in the emission region.[5] It is generally accepted[2,6] that residual gases are the foremost contributors to the degradation of the phosphor material and device reliability, and are as well linked to poor brightness uniformity.[7]

We have previously shown that the change of the pumping direction from longitudinal to transverse increases the vacuum conductance of the display, and makes it independent of the anode–cathode separation.[3,4] One way to change the pumping direction is to use porous emitters instead of the conventional Spindt tips, so that the pores also operate as an escape path for the gases through the cathode plane. In Ref. 3 we have shown that the edge of a metallic ''*volcano-type*''
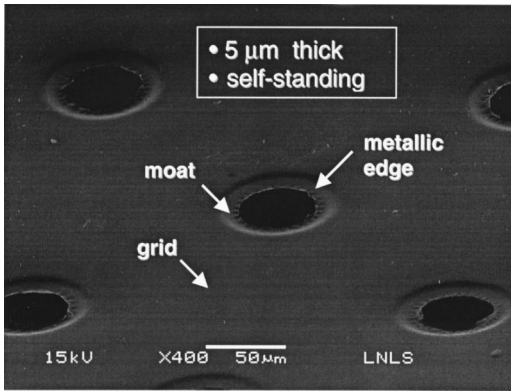
FIG. 1. SEM image of a polyimide porous membrane.

FIG. 2. SEM image of a star shaped pore in a polyimide porous membrane.

pore features a field enhancement factor at least as large as for metallic edges with equivalent geometry parameters. Our experiments also show that pore edges in a diamond membrane perform as well as field emitters.

Despite its promising emission characteristics, the use of diamond membranes for field emission is limited by difficulties in producing large area diamond films. Indeed, freestanding diamond membranes larger than 4 in. are difficult to produce. In addition, the surface of the diamond film displays considerable corrugation on the ''as-deposited'' side, and high resolution patterning of the film is thereby difficult. Consequently, it is necessary to find a substitute to diamond for the production of freestanding porous membranes for field emission display applications. In this work, we present porous emitters using freestanding polyimide membranes coated with a metal layer, analogous to the approach previously used for porous diamond emitters.[3,4] The processing methodology and, in particular, the optical patternability of polyimides are suitable for large area applications. The vacuum compliance of polyimide is still poorly understood, especially in the context of field emission applications. However, polyimide is commonly accepted as being highly vacuum compliant.

In this article we present electron emission data from polyimide porous membranes measured in a diode configuration, with circular porous geometry. In addition, we propose a new triode configuration based on the use of a polyimide porous membrane with predefined pore geometry to maximize the emission properties. Feasibility of such a pore geometry is demonstrated. Finally calculations regarding focusing issues of this triode geometry are carried out.

II. EXPERIMENT

Freestanding polyimide membranes are built following the usual steps of optical lithography: spinning, UV exposure, developing, curing, and liftoff. Following this procedure we are able to produce freestanding membranes as large as 3 in. However, we anticipate no restrictions in producing larger membranes. Figure 1 shows a SEM image of pores in a polyimide membrane. The diameter of the pores is 40 μm, the distance between pores is 200 μm, and the membrane thickness is 5 μm. These are largely independent parameters:

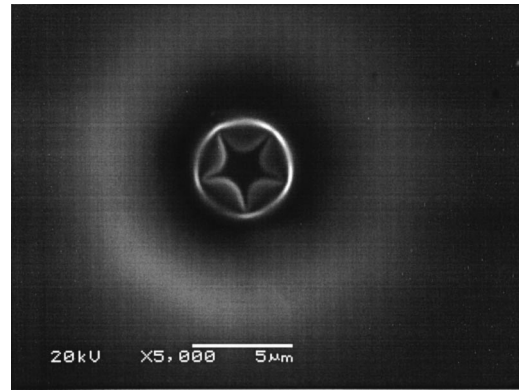in other samples we were able to produce pores as close as 30 μm without drastically compromising the overall mechanical stability. Pores in a variety of shapes can be produced as well, and the star-shaped pore in the polyimide membrane shown in Fig. 2 illustrates the flexibility of the method.

Coating the polyimide membrane with a metal film forms the cathode. The coating was obtained using metal plasma immersion ion implantation and deposition (MePIIID),[8] which was chosen for its excellent vertical wall coating and adhesion characteristics. The inner walls of the pores must be metal coated to fabricate the geometry shown in Figs. 3(b) and 3(c). MePIIID is a deposition process based on filtered pulsed arc plasma, in which ion implantation or simple depo-
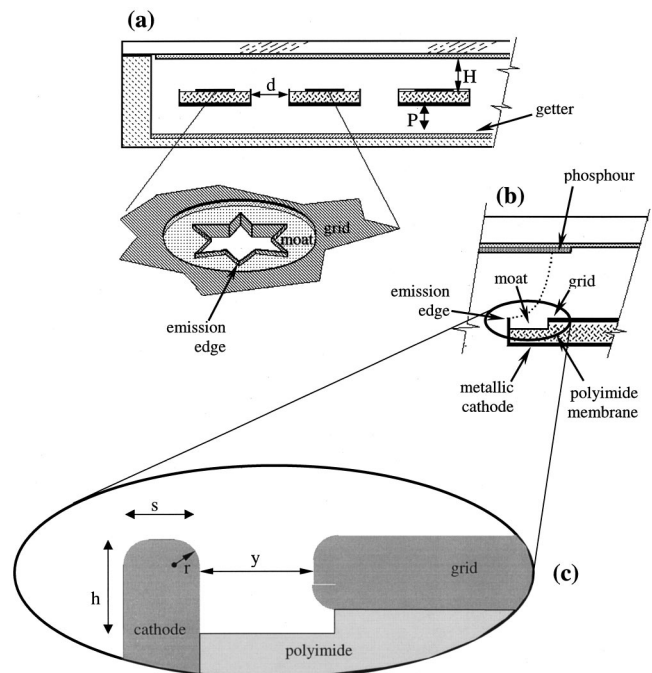

FIG. 3. Schematic of a field emission display based on porous emitters: (a) side view of the anode, cathode and back plate structure, (b) emitter profile; the dotted line illustrates the approximate electron trajectories (c) detail of the cathode tip used in the simulations, with a curvature radius r, and width s.

sition can be achieved depending on the choice of the bias voltage applied to the sample. In the case of electrically insulating materials (such as polyimides), it is not possible to uniformly bias the sample surface during early deposition stages. However, if the deposited material is conducting, this problem is overcome after a thin layer has been deposited, and bias can be used to induce ion implantation, which leads to better adhesion. Stress is a concern in films produced by MePIIID since it causes curling of the freestanding polyimide membrane. We have used a hard frame to maintain the planarity of the membrane.

Preliminary field emission measurements were performed in a diode configuration. The measurements used the approach curve method, which yields the electric field necessary to produce a given threshold current (3 nA in this work); see Ref. 9 for a detailed description of the method.

We addressed some of the triode configuration focusing issues numerically. Using a two-dimensional model,[10] we considered geometric effects on the size and location of the light spots created by electrons hitting the anode. We solved the electrostatic problem using the boundary element method,[10,11] which allows for the calculation of the electric field and potential at any point of the device. The method does not require the use of a grid, but only the discretization of the boundaries. This feature is essential in simulating field effect devices because very dissimilar length scales must be taken into account in order to obtain accurate results. Our electron emission model evaluates the current density at the cathode surface from the tunneling transmission coefficient, which is obtained from the solution of the one-dimensional open boundary Schrödinger equation. The potential barrier includes the effect of image charges and nonuniform electric fields. The current density is used to calculate the rate of electron emission for each segment of the emitter's surface. The emission time is assumed to follow a Poisson distribution. The electron's velocity magnitude and angle with the normal to the surface are also stochastically generated following the probability distribution of field emitted electrons. Ballistic transport is used to propagate electrons through the device.

III. RESULTS AND DISCUSSION

The approach curves showed in Fig. 4 were obtained for two different pore densities: 1111 pores/mm^2 (dense), and 123 pores/mm^2 (sparse). The electric field necessary to produce an anode current of 3 nA was 6.9 and 12.7 V/μm, respectively, and the current per pore was ~1 and 10 pA, respectively, for the electric fields mentioned above. The experimental setup was in a diode configuration, that is, a circular pore with no grid. The geometry of the pores is described in Fig. 1. We did not submit the polyimide membrane sample to O_2 etching, neither DLC coating, so its geometry is equivalent to that of the diamond membrane in Refs. 3 and 4, and therefore their performances can be qualitatively compared. Also, to make the comparison possible, circular pores were patterned in the polyimide membranes.
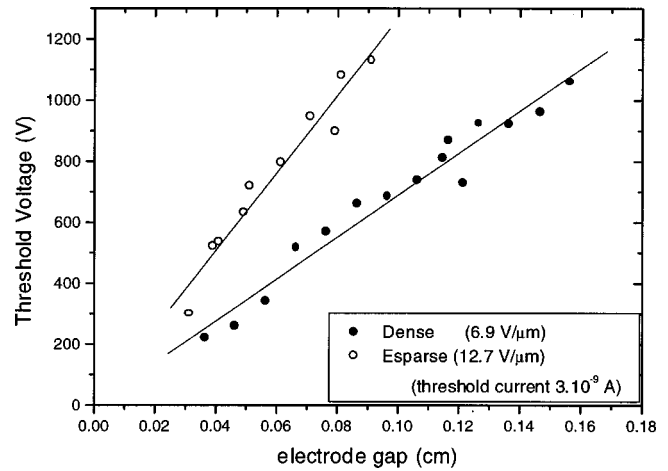

FIG. 4. Approach curves for two polyimide membranes with different pore densities.

Figure 4 clearly indicates that a higher concentration of circularly shaped pores results in better emission, since the slope of the corresponding approach curve is smaller. In other words, a smaller electric field was necessary to obtain the threshold current of 3 nA. This fact strongly suggests that the emission takes place at the pore edges.

We can now compare the current per pore obtained from polyimide membranes with that obtained from diamond membranes. Diamond performs better, as one would expect, showing currents per pore about 10–30 times larger for electric fields in the range of 7 V/μm. Such difference could be attributed to the diamond's suggested negative electroaffinity,[12] to the lower work function for diamond than for molybdenum, to the presence of gases adsorbed to the surface of the emitters in both cases, or to slight variations of the cathode's curvature radius. The introduction of a moat around the pore combined with DLC coating could possibly improve the emission properties of the polyimide membranes, as a result of the removal of dielectric material from regions close to the edge and because of the good emission properties of DLC, respectively.

An evolution from the concept presented in Refs. 3 and 4 is the use of a star-shaped pore, instead of a circular one. The star-shaped design leads to a three-dimensional field enhancement, while in the circular design, the field enhancement is essentially two dimensional. Therefore, if the emitter curvature radii are the same in both designs, the field at the emitter edge will be approximately three times larger in the star-shaped design,[8] allowing for lower gate voltages. The device proposed here includes a grid in the triode configuration. Figure 3(a) shows the star-shaped version of the device we are proposing and Fig. 3(b) shows a transverse section with the cathode emitter and the grid.[13] Figure 3(c) shows the profile used in our simulations. We have used uncoated molybdenum emitters for the experimental part of the work, although coating the emission edges with, e.g., diamond-like carbon is possible and might improve the emission properties of our device.[3,14]

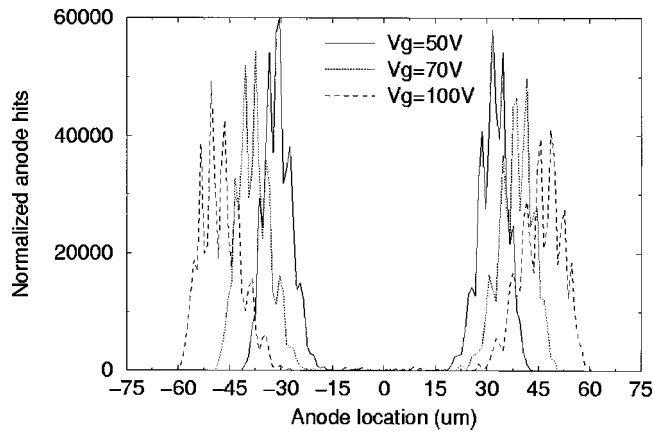Producing a cathode-grid structure as shown in Fig. 3 is

FIG. 5. Electron hits in the anode for different voltages applied to the grid. The jagged nature of the peaks is an artifact of the calculation, and results from the finite number of segments used to discretize the cathode tip. The zero in the *x* axis marks the point in the anode vertically aligned to the center of the pore. Star edge to grid separation $y = 0.5$ μm.

FIG. 6. Electron hits in the anode for different pore sizes *d*. Star edge to grid separation $y = 0.5$ μm.

difficult because the geometric center of the grid circle has to coincide with the geometric center of the pore. Conventional lithographic alignment techniques lack the required precision. As we will show later, a small misalignment results in a source of emission nonuniformity, in addition to variations in the curvature radius along the pore edge. A self-aligning process based on capillarity effects was used to fabricate the triode structures.[15] The moat between the grid and the cathode can be achieved by using oxygen plasma etching, and by using the metal grid as a mask. Notice however that metal oxidation may occur during this process possibly changing the emitting properties of the metal surface.

The computer simulations of the triode configuration provide a qualitative description of the device's focusing characteristics with respect to the pore size, gate voltage, and grid-pore alignment. In all the calculations described below we used the following parameters: polyimide dielectric constant $\epsilon = 2.9$, cathode height $h = 5$ μm, cathode curvature radius $r = 5$ nm and width $s = 50$ nm, cathode–anode separation $H = 200$ μm, and cathode-back plate separation $P = 100$ μm [see Figs. 3(b) and 3(c)]. The anode voltage was set at 5 kV.

Figure 5 shows the normalized electron hits on the anode (unit area under each curve) for different gate voltages. Because the gate voltage pulls electrons out of the cathode tip and away from the center of the star, the area on the anode immediately above the pore is not illuminated, but only an annular region. The radius of the annular region ranges from 70 to 100 μm for an anode–cathode separation of 200 μm, while its width is of the order of 25 μm. The radius of the annular region is weakly dependent on the anode–cathode separation *H* since it scales as the square root of *H*. Thus, illuminating the entire anode area is a concern in this design, even if emission nonuniformity issues can be solved. There are, however, many possibilities to explore, e.g., increase the density of pores in order to achieve an overlap of the spots on the anode.

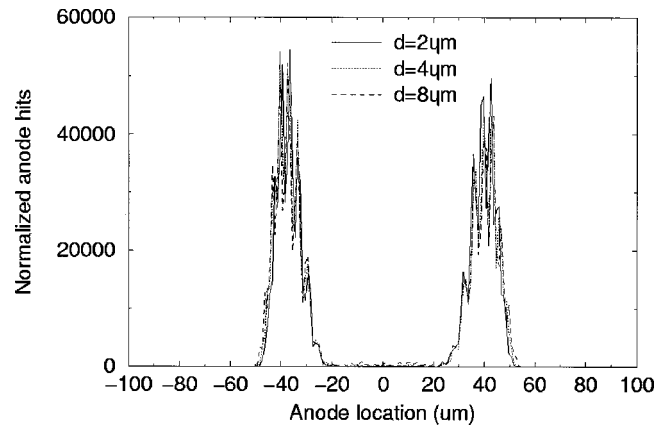Figure 6 shows the electron hits on the anode for different

pore sizes *d* [see Fig. 3(a)]. The radius of the annular region formed at the anode is weakly dependent on the pore size and there is no relevant screening due to interaction between the different edges of the star down to a separation $d = 2$ μm.

Finally, we kept the distance between one of the star edges to the grid at 0.5 μm, while the other grid–edge separation *y* was varied between 0.5 and 1 μm. Figure 7 shows that a misalignment of 10% corresponding to $y = 0.6$ μm (50 nm off the pore center), results in a highly nonuniform emission pattern. Therefore, a good grid-pore alignment, better than 10% of the moat width, is an essential ingredient for uniform field emission from our devices.

IV. CONCLUSIONS

Porous circular or star-shaped field emission devices can be produced using freestanding polyimide membranes. The use of MePIIID deposition process is capable of coating the membrane with an appropriate metal film. Special attention has to be given to the stress induced in the polyimide membrane after metal deposition. Field emission measurements
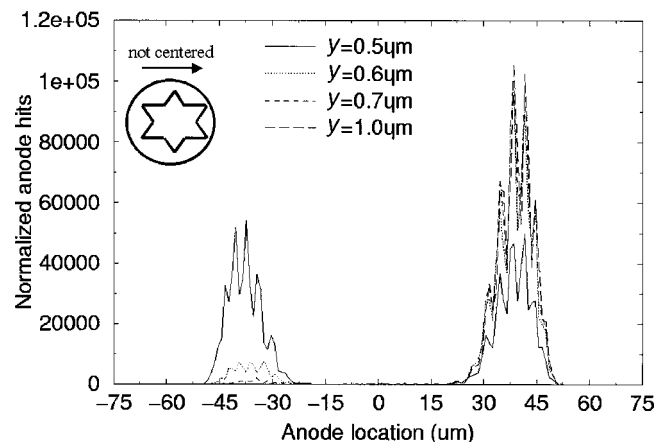

FIG. 7. Electron hits in the anode for a variable grid-pore alignment. The star edge to grid distance was kept constant ($y = 0.5$ μm) for one of the six edges while it was varied for the edge diametrically opposed.

from porous polyimides coated with metal in a diode configuration showed that the current emitted is about 10–30 times smaller than the current obtained from porous diamond membranes.[3,4] However, polyimide membranes offer several fabrication advantages over porous diamond membranes which, we believe, compensate for the smaller emission current. We observed that the emission current is dependent on the pore density, showing that the pores are the source of electron emission.

Computer simulations of electron trajectories in a triode configuration showed that the illuminated area has a weak dependence on gate voltage and size of the pore, while the device emission uniformity is very sensitive to grid-pore alignment.

ACKNOWLEDGMENTS

[1]B. R. Chalamala, Y. Wei, and B. E. Gnade, IEEE Spectrum **35**, 42 (1998).
[2]P. H. Holloway, J. Sebastian, T. Trottier, S. Jones, H. Swart, and R. O. Petersen, Symposium H, Flat Panel Display Materials, Spring Meeting Symposium Proceedings, Materials Research Society, 1996.
[3]V. P. Mammana, F. T. Degaspari, O. R. Monteiro, J. H. Vuolo, M. C. Salvadori, and I. G. Brown, J. Vac. Sci. Technol. B (accepted).
[4]V. P. Mammana, S. Anders, O. R. Monteiro, and M. C. Salvadori, J. Vac. Sci. Technol. B **18**, 2415 (2000).
[5]Y. R. Cho, H. S. Kim, J. D. Mun, J. Y. Oh, H. S. Jeong, and S. Ahn, J. Vac. Sci. Technol. B **16**, 3069 (1998).
[6]J. S. Sebastian, H. C. Swart, T. A. Trottier, S. L. Jones, and P. H. Holloway, J. Vac. Sci. Technol. A **15**, 2349 (1997).
[7]D. Temple, Mater. Sci. Eng., R. **24**, 185 (1999).
[8]A. Anders, Surf. Coat. Technol. **93**, 158 (1997).
[9]S. Dimitrijevic, J. C. Withers, V. P. Mammana, O. R. Monteiro, J. W. Ager III, and I. G. Brown, Appl. Phys. Lett. **75**, 2680 (1999).
[10]L. R. C. Fonseca, P. Von Allmen, and R. Ramprasad, J. Appl. Phys. **87**, 2533 (2000).
[11]P. A. Knipp and T. L. Reinecke, Phys. Rev. B **54**, 1880 (1996).
[12]F. J. Himpsel, J. A. Knapp, J. A. Van Vechten, and D. E. Eastman, Phys. Rev. B **20**, 624 (1979).
[13]Patent submitted to the Brazilian Patent Office, INPI (2000).
[14]F. Y. Chuang, W. C. Wang, F. Cheng, C. Y. Sun, and I. N. Lin, J. Vac. Sci. Technol. B **15**, 2072 (1997).
[15]Disclosure of Invention, Lawrence Berkeley Laboratory, CA.